STRUCTURAL OPTIMIZATION OF A HAT-STIFFENED PANEL USING RESPONSE SURFACES

Roberto Vitali, Oung Park, Raphael T. Haftka, and Bhavani V. Sankar

University of Florida

Department of Aerospace Engineering, Mechanics and Engineering Science

Gainesville, FL 32611-6250

Cheryl A. Rose

NASA Langley Research Center

Structural Mechanics Branch

Hampton, VA

Abstract

This paper describes a design study for structural optimization of an upper cover panel of a typical passenger bay of a blended wing body transport airplane. For these type of airplane the structure that obtained a common consent among designers is a sandwich structure. However unresolved issues of sandwich structures, like core crushing, might prevent their employment and suggest the study of an alternative all composite structure. A hat-stiffened laminated composite panel concept is considered as an alternative to the sandwich configuration. The initial geometry of the hat stiffener configuration is determined with the PANDA2 program by restricting the design to uniform axial properties. Because of pressure loading, a more efficient design has variable properties. Such designs are obtained by combining the STAGS finite element program with the optimization program in the Microsoft EXCEL spreadsheet program using response surfaces. Buckling and stress response surfaces are constructed from multiple STAGS analyses and are used as optimization constraints. The optimization conducted with the response surfaces results in considerable weight savings compared to the uniform cross-section design, albeit at the

expense of a more complex design. Moreover, after the initial optimization cycles are performed a subdomain of the design space is identified where simple approximate analyses, such as Euler-Bernulli beam theory and Kirchhoff plate theory applied to laminated composites, can be used to predict the behavior of the structure.

Introduction

Major air carriers have expressed the need for larger airplanes to meet the growing demands for air travel, especially in the pacific rim and on transatlantic routes between major airports in the USA and in Europe. A blended wing body (BWB) 800 passenger aircraft is one of several configurations currently being considered for satisfying this need. As the name implies, a principal feature of a BWB transport is a wide double deck centerbody which is blended into the wing. Due to the shape of the airplane, the pressurized centerbody region, which includes both the passenger area and the cargo area, is non-circular (see Fig. 1). The non-circular centerbody region is challenging from the standpoint of structural design, since the upper and lower cover panels carry the overall aircraft body loads and moments (N_y and M_x in Fig. 1), internal pressure, and running loads due to wing bending (N_x and M_y in Fig. 1). To reduce instability problems in the upper cover panel, which is subjected to compressive wing bending loads, and to reduce bending stresses due to the internal pressure loading, the inboard centerbody section is divided into several bays separated by chordwise ribs. A typical passenger bay is 150 inches wide, as shown in Fig. 1.

A variety of structural configurations for the pressurized cover panel structure have been considered as part of a BWB design study, led by the McDonnell Douglas Corporation (now Boeing Company Corporation) in collaboration with NASA and four universities (University of Florida, Stanford University, University of Southern California, and Clark Atlanta University). The configurations that have been considered include conventional skin-stringer constructions, deep sandwich structure, and separate structures for carrying the internal pressure and wing bending loads. A deep sandwich configuration for the structure of the was the preferred design concept among the designers. However some unresolved issues of sandwich structures might

prevent their employment as primary structure for the BWB. The present paper describes a structural optimization study of one of the alternative structural concepts being considered for the upper cover panel of a typical passenger bay of a BWB transport airplane. Specifically, results are presented for a composite hat-stiffened skin panel configuration. The skin and all of the components of the hat-stiffener are built up from graphite-epoxy, warp-knit preforms. Each preform is a stack of material equivalent to seven layers of unidirectional prepreg with 0, 45 and 90 degree fibers, and has a cured thickness of 0.055 inches. The loading cases used in this preliminary study did not include N_y and M_x shown in Fig. 1 and the wing bending moment M_y was transformed in equivalent N_x compression and tensile loads running in the upper and lower panels. A comparison on the weight of the cover panel obtained from different structural concepts could be obtained from the load cases furnished by McDonnell-Douglas and used in this study. In particular a design was considered to be a valid alternative to the sandwich one if it reached a weight of 3.0 lb/ft^2.

The structural optimization problem is formulated using the panel weight as the objective function, with stress and buckling constraints. The spacing of the hat-stiffeners, the thickness of the skin, and the thickness of the components of the hat-stiffener are used as design variables. The thickness variables are integer multiples of the basic composite material stack described above. Therefore, the optimization problem is discrete. Furthermore, the structural analyses required to evaluate the constraints are performed by an analysis code that does not have optimization capabilities and is difficult to interface with an optimization program. For such situations, response surface techniques, which create simple approximations of structural response, have been shown to be useful[1]. Response surface techniques also permit simple analysis models to be integrated with more complex analysis models. In the present work, both simple and complex analysis models are integrated in response surfaces that are used in the structural optimization. A flow chart of the different hat stiffener structures obtained during the optimization procedure is shown in Fig. 1A.

Problem Description

The structural configuration considered in the optimization problem is a hat-stiffened skin, upper cover panel of a typical passenger bay, as shown in Fig. 2. The panel is 150 inches long in the spanwise (x) direction, and 900 inches long in the chordwise (y) direction. Two loading conditions are considered in the design. The first loading condition is combined internal pressure and spanwise (x) compression. The second loading condition is internal pressure only. The two load cases considered do not have a load component in the chordwise direction. The ends of the stiffened panel at $x = 0$ inches , and at $x = 150$ inches are clamped. The clamped boundary condition is achieved by two simple support boundary conditions applied to the base and to the crown of the stiffener. The end of the panel at $x = 0$ inches is restrained from movement in the x-direction while the opposite end of the panel at $x = 150$ inches is constrained to have a uniform u displacement. The unloaded edges of the panel at $y = 0$ inches and at $y = 900$ inches are simply supported with the v displacement component unconstrained.

The skin and the individual components of the hat stiffener are constructed from graphite-epoxy preforms, which were developed under several NASA Contracts.[2] Each preform is a stack of material equivalent to seven layers of unidirectional prepeg with 0, 45 and 90 degree fibers. The nominal stacking sequence of the preforms used in the skin and in all of the components of the hat-stiffener is [45/-45/0/90/0/-45/45]. Each preform, or stack, has a cured thickness of 0.055 inches. Nominal material properties for a cured stack, and the stress allowables that are used in the designs, are provided in Table 1.

Structural Optimization

An initial optimum structural design for the upper cover panel was obtained using the PANDA2 program[3]. A refined optimum structural design was then obtained by an optimization using response surface techniques. The analyses required to construct the response surfaces were performed using both simple and complex analysis models. The complex structural analyses were performed using the STAGS (Structural Analysis of General Shells)[4] finite element program. The

initial design was obtained for a combined load case of 14.84 psi internal pressure, and spanwise compression N_x = *-4319 lb/in*. The loadings applied for the initial design did not include N_y, M_x and M_y components. These simple loadings were considered sufficient by McDonnell-Douglas to obtain an indication on the quality of a preliminary design concept for the upper cover panel. The optimization for the initial load case is described herein in the sections "Design Using PANDA2 for Initial Load Condition" and "Design Using Response Surface Techniques for Initial Load Condition." As the airplane design evolved, the design loads for the combined load case were updated to *p = 15.59 psi* and spanwise compression N_x = *-2879 lb/in*, and an additional load case of internal pressure only (*p = 18.56 psi*) was added. The optimum structural design obtained for the initial load case was used as the starting point in the optimization problem for the updated load conditions. The design for the updated load conditions is described herein in the section "Design for Updated Load Conditions."

Design Using PANDA2 for Initial Load Condition

The first step in the structural optimization was to use the PANDA2 program to obtain an initial design. PANDA2 was developed specifically to find minimum weight designs of stiffened, flat or curved panels, or complete cylindrical shells made of laminated composite materials. The stiffeners may run in one, or in two orthogonal directions. All stiffeners in one direction are assumed to be identical and uniformly spaced. For the typical stiffener PANDA2 finds the spanwise location in which each element of the panel module has the highest compressive stresses, and performs a stability analysis based on these values. The results of the stability analysis are then used to size each element of the panel module.

In the present problem, the stiffeners run in the spanwise (*x*) direction, and the panel consists of repetitive modules in the chordwise (*y*) direction. Furthermore, the properties of the panel are assumed to be uniform in the spanwise (*x*) direction. The cross-section of a panel module and the design variables used in the PANDA2 optimization are shown in Fig. 3. A single module consists of a stiffener, plus the panel skin, with width equal to the spacing between

stiffeners (*b* in Fig. 3). PANDA2 obtains buckling load factors employing closed form expressions and inexpensive finite difference analyses of a descritized panel module. The optimum design obtained by PANDA2 always features continuous design variables, however the thickness of the panel skin and the thickness of the individual components of the hat-stiffener are discrete variables, since the thicknesses are limited to integer multiples of the basic material stack. Therefore the optimum design obtained by PANDA2 has to be rounded to the next feasible value of the discrete design variables.

The objective function, the design variables and the side constraints used in the PANDA2 optimization are listed in Table 2. The first constraint ensures that there are enough equally spaced stiffeners in the panel for a single module model to give a good approximation to the local skin buckling mode. The second and third constraints are recommended by the PANDA2 user's guide to guarantee numerical stability in the solution procedure. The fourth constraint controls the height of the hat, where the upper value reflects a manufacturing limit. The fifth and sixth constraints ensure that the flanges are at least 1.3 inches wide, again for manufacturing reasons, and the seventh constraint ensures that the hat-stiffeners have reasonable proportions. Finally, the eighth constraint sets the upper and lower thickness bounds of the panel skin and of all elements of the hat-stiffener. Additional constraints on the design included global and local buckling, crippling, stiffener pop-off, maximum stresses along and normal to the fibers in each lamina, and maximum in-plane shear stresses within each element of the stiffener. In evaluating the constraints, a factor of safety equal to 1.3 was applied to the stresses and a factor of safety equal to 1.15 was applied to the buckling load factor. The buckling load safety factor reflects a design requirement that the structure will not buckle between design limit load and design ultimate load.

As shown in Table 3, the optimum design obtained by the PANDA2 program weighed 4.65 lb/ft^2. Rounding off the thicknesses to the nearest discrete thickness raised the weight to 4.8 lb/ft^2. In Table 3 the design obtained from PANDA2 and the design obtained by rounding the thicknesses are shown. For the rounded off design shown, the active constraints at the mid-length of the panel were fiber compression in the crown, web buckling, and axial (spanwise direction) strain in the crown. At the ends of the panel, the active constraints included local buckling of the

panel skin between the hat-stiffeners, local buckling of the panel skin under the hats, and spanwise compression in the panel skin.

Design Using Response Surface Techniques for Initial Load Condition

For the loading and boundary conditions of the current problem, the design obtained with PANDA2 is conservative. The conservative design results from the imposed requirement that the panel properties are constant in the spanwise direction, while the loading for the present problem is variable in the spanwise direction.

A more efficient design for the stiffened panel was obtained by allowing the cross-section of the panel to vary in the spanwise direction. Based upon the results of the PANDA2 analysis, the panel was divided into three sections: two identical sections at the ends of the panel, and a section in the interior of the panel, as shown in Fig. 4. The tendency of the skin to buckle near the ends of the panel, which was an active constraint in the PANDA2 analysis, was reduced by adding a layer of material equal to the thickness of the flange to the panel skin between the hat stiffeners and to the panel skin under the hat-stiffeners. Furthermore, the thickness of the crown of the hat stiffeners in the end sections of the panel was allowed to be different than the thickness of the crown of the hat stiffeners in the interior region of the panel. The cross-sections of a panel module at the ends of the panel and in the interior region of the panel are shown in Figs. 5a and 5b, respectively.

The STAGS[4] program was used to obtain accurate buckling loads and stress predictions for the variable cross-section panel shown in Figs. 4 and 5. STAGS is a finite element code for the non-linear analysis of general shell structures of arbitrary shape and complexity. STAGS, however, does not have an optimization capability. Response surface techniques, which create simple approximations of structural response, have been shown to be useful for design optimization when the design variables are discrete and when it is difficult to integrate the analysis and optimization codes. Response surface methodology is used to obtain a relationship between a specified response variable (dependent variable) and the design (independent) variables. The response surface model describes this relationship. In the current study, STAGS finite element

analyses were used to construct response surface models to approximate the panel buckling response and to approximate the compressive, spanwise, skin stress at the thickness discontinuity between the end and the interior regions of the panel. For the first loading condition considered this study, the thickness discontinuity was the only region in the hat stiffened panel where the stress constraint was violated. The response surfaces created were then used as constraint functions in an optimization procedure to minimize the panel weight. The optimization was performed using a spreadsheet in the Microsoft EXCEL[5] software program that allows discrete design variables. The optimization module in EXCEL, called "SOLVER" is available in several other spreadsheet programs. The design variables used in the optimization are given in Table 4. The thickness of the flange (t_f = 0.11 in.) and the thickness of the web (t_w = 0.22 in.) were kept constant during the optimization process.

Both the buckling response surface and the stress response surface were approximated using polynomials. A least squares estimate of the unknown coefficients in the polynomials was obtained by evaluating the structural response (panel buckling load or stress at the thickness discontinuity) at a number of design points that exceeded the number of coefficients in the approximating polynomials. The structural response at the individual design points was determined using the STAGS finite element code. In all of the STAGS analyses, an additional factor of safety equal to 1.25 was applied to the end load so that a load of 5398 lb./in was used.

In order to keep the cost of constructing a response surface as low as possible, while ensuring the accuracy of the response surface model, care must be taken in selecting the design points. Several methods are available for selecting the design points so that the error in the approximation is minimized. In the present study, the D-Optimality criterion[6], as implemented in the JMP program[7], was employed to select the design points. The implementation in the JMP program finds a D-Optimal set of points from a given set of candidate design points in the design domain. The 9604 candidate design points that were used for constructing the response surfaces are defined in Table 5. Also given in Table 5 is a nominal design, selected by engineering judgment. The nominal design weighs 3.741 lb/ft^2, has a buckling load factor of 1.898, and has spanwise, compressive skin stress at the thickness discontinuity equal to 20,288 psi.

Before proceeding with the selection of the design points, the size of the design domain was reduced from 9604 to 740 feasible design points by introducing the following constraints based on the expectations for the optimum design:

- The weight was required to be between 3.0 lb/ft^2 and 4.3 lb/ft^2.
- The skin near the ends of the panel was required to be thicker than the skin in the interior of the panel ($t_{sm} \leq t_{sb}$).
- The crown in the interior of the panel was required to be thicker than the crown near the ends of the panel ($t_{cb} \leq t_{cm}$).

Buckling Response Surface. The STAGS model used in the analysis of the stiffened panel had approximately 70,000 degrees of freedom. The panel skin and all of the elements of the stiffeners were modeled as branched shells. One linear stress and linear buckling analysis using this model required approximately 6,500 CPU seconds on a DEC ALPHA 200 4/166 work station.

Because of the time required to perform each of the structural analysis, a simple linear polynomial response surface for the buckling load factor was constructed first using 11 design points (design points 1-11 in Table 7 of Ref. 8). Ten of the design points (design points 2-11) were selected using the D-Optimality criterion. Design point 1, the nominal design given in Table 5, was selected by engineering judgement. The linear fit, constructed using these 11 points spanning through the entire design domain, for predicting the buckling load factor was very poor with an estimate of the root mean square error (RMSE) = 0.61, and $Ra^2 = 0.046$. As the buckling load factor is approximately to 1.0, this error is very large. The parameter Ra^2 indicates the goodness of a fit. A perfect fit is indicated by $Ra^2 = 1.0$, and $Ra^2 = 0.0$ represents a very poor fit.[6]

In an attempt to improve the accuracy of the response surface, a new design domain was defined around the nominal design. The thickness variables were permitted to change by $\pm$0.055 inches from the nominal design and the length of the end section, d, was permitted to change by $\pm$12 inches. Thus, each variable could have 3 possible values and a total of 243 design points was

generated (81 of the generated points violated the t_{sm} thickness constraint since the nominal design was at the lower bound for this design variable). Twelve design points were selected out of these 243 points using the D-Optimality criterion. (points 12-23 in Table 7 of Ref. 8.)

The linear response surface for the buckling load factor obtained using the 12 new points had an RMSE = 0.54 and $Ra^2 = 0.56$, indicating that the fit was still unsatisfactory. Moreover, the t-statistics of the coefficients were very small. The t-statistic[6] is a parameter that indicates the confidence in the values of the coefficients obtained. A higher confidence is indicated by a higher value of the t-statistic.

Since the linear response surface models were not satisfactory, 10 design points were added to the 23 design points that were used in constructing the two linear response surface models described above. Using these 33 design points (Table 7, Ref. 8), a full quadratic polynomial was fitted over the entire design domain. A full quadratic polynomial in 5 design variables has 21 coefficients. Terms in the polynomial with a low t-statistic were discarded as long as Ra^2 kept increasing. The quadratic polynomial retained ten coefficients, and is given by:

$$\begin{aligned} l = & -4.199 + 0.1708\ d + 34.14\ t_{sm} - 0.001362\ d^2 - 31.98\ t_{sb}{}^2 - 0.4712\ d\ t_{sm} \\ & + 72.30\ t_{sm}\ t_{sb} - 95.94\ t_{sm}{}^2 - 0.759\ t_{cm}\ d + 22.43\ t_{cm}\ t_{sb} \end{aligned} \qquad (1)$$

For the polynomial fit in Eq. (1), RMSE = 0.25 and $Ra^2 = 0.82$. Furthermore, the lowest t-statistic was 3.17, which indicates reasonable confidence in the coefficients. The accuracy of the response surface was also checked by constructing several response surfaces using only 32 points, and then comparing the response surface predictions at the point left out with the STAGS analysis predictions at that point (a procedure known as PRESS[6]). Based upon these comparisons, the quadratic response surface prediction for the buckling load factor is expected to have less than 20% error.

Stress Response Surface. A quadratic response surface for the compressive, spanwise stress in the skin, at the change in skin thickness between the end sections of the panel and the

interior section of the panel, was also constructed. Stress values at all other locations in the panel, for all of the designs analyzed, did not exceed the maximum stress allowable. The response surface obtained with units of (ksi) is given by:

$$s = 1.087 - 2.011\,d - 95.15\,t_{sb} - 48.15\,t_{sm} + 0.01503\,d^2 - 1.141\,d\,t_{sb} + 2.816\,t_{sm}\,d + 32.34\,t_{sm}\,t_{sb} + 81.36\,t_{sm}^2 \qquad (2)$$

with, $Ra^2 = 0.96$ and RMSE = 1924 psi. The t-statistics for all of the coefficients were higher than 3.33. The accuracy of the response surface was also checked by the PRESS procedure, which indicated that a maximum error of 20% is expected when the stress response surface is used to estimate the compressive, spanwise stresses in the skin near the thickness discontinuity.

Optimization Using the Response Surfaces. As indicated above, the response surface for the buckling load factor, λ, and the stress response surface had errors of 20%. Therefore the required buckling load factor was increased by 20% from 1.15 to 1.38 and the safety factor on the compressive stresses was increased by 20% from 1.3 to 1.56.

The optimization problem was formulated as shown in Table 6 and solved using a reduced gradient optimizer available in Microsoft EXCEL. The optimum design obtained, subject to the constraints specified in Table 6, is presented in Table 7. Analysis of the design in Table 7 with STAGS gave a buckling load factor, $l = 1.379$, and a maximum spanwise, stress, $s = -22{,}450\ psi$, in the skin at the boundary between the end section and the interior section. The variable cross-section design for the upper cover panel, obtained using the response surface approach has a weight of 3.53 lb/ft^2 (Table 7) compared to a weight of 4.86 lb/ft^2 (Table 3) for the uniform panel design cross section.

Design for Updated Load Conditions

After the optimization described above was completed, the design loads were updated as the overall airplane design changed. A new load case of internal pressure only ($p = 18.56\ psi$) was

added, and, in the combined load case, the pressure loading was changed from 14.84 psi to 15.59 psi and the in-plane, spanwise load was changed from 4319 lb/in to 2879 lb/in. In addition, the buckling and stress safety factors were reduced to 1.0. The reduction in the buckling safety factor reflected a change in design philosophy, allowing local buckling of the skin between the design limit load and the design ultimate load.

When PANDA2 was used to optimize the hat stiffener panel with uniform cross-section for the updated combined load case a panel with a weight of 4.30 lb/ft^2 was obtained, indicating a less severe loading condition then the initial loading condition one. Moreover, Dr David Bushnell, the developer of PANDA2 obtained an optimal two cross-section hat stiffener panel using his program. For a transition specified at distance of 24.0 inches the weight obtained by PANDA2 was 3.71 lb/ft^2.

However a more precise analysis tool was desired and therefore STAGS was employed again. The STAGS finite element model of the hat stiffened panel was simplified to include only one panel module, 13.83 inches wide, with symmetry conditions imposed along the sides parallel to the x-axis. Also, the weight calculations were refined to remove duplications in the previous calculations due to intersecting finite elements.

The design for the updated load conditions was initiated using the optimum design obtained in the design cycle for the initial load condition as a starting point. In the preceding optimization, the thickness of the skin in the interior section of the panel, t_{sm}, remained at its lower limit throughout the optimization process, and was not an active variable in the design. In addition, for the optimum design presented in Table 7, the webs account for approximately 40% of the total panel weight. Based upon these observations, the design variable list was modified by including the web thickness, t_w, as a design variable and by removing the thickness of the skin in the interior section of the panel, t_{sm}, from the design variable list.

A design domain for the updated optimization was generated around the optimum design point obtained in the previous optimization (design point number 1 in Table 8). The design domain was limited to 162 new design points by introducing the following restrictions. The thickness of the skin in the end sections of the panel, and the thickness of the crown in the interior

section of the panel, were permitted to change by $\pm$0.055 inches from the previous optimum design (Table 7). The thickness of the crown in the end sections of the panel was allowed to be twice as thick as it was for the initial load case in order to deal with the new load case of internal pressure only that induces high tensile stresses in the crown near the panel ends. The web was constrained to have a thickness equal to 0.165 inches or 0.220 inches. A thinner web would violate the buckling constraint and a thicker web would result in unacceptably heavy designs. The distance from the panel ends to the thickness discontinuity, *d*, was permitted to change by $\pm$ 6 inches from the previous optimum design value. The thickness of the skin in the interior section of the panel, t_{sm}, was equal to 0.110 inches, and was held constant during the optimization process. The flange thickness was equal to 0.110 inches was also held constant during the optimization process.

The JMP program was employed to select a D-Optimal set of 25 new design points from the 162 candidate design points. STAGS was used to conduct linear analyses of each of these 25 designs for the internal pressure only load case and for the combined load case. Table 8 shows the 25 designs and the buckling load factors obtained from STAGS for the internal pressure only load case, λ_p, and for the combined load case, λ_c. The buckling load factors were obtained from a linear bifurcation analysis. For the combined load case, the internal pressure load and spanwise compressive load were included on one load set. The pressure only load generated high tensile stresses in the crown of the hat stiffener due to bending. The tensile spanwise stresses in the crown, calculated at 3.5 inches from the panel end, for the internal pressure only load case, are also provided Table 8. Stress calculations were not performed for all of the designs. The design points where stress data is not available have dashes in the maximum stress column in Table 8.

The stress calculations performed with STAGS indicated that the stress allowable was exceeded only in the crown of the hat-stiffener, for the internal pressure only load case. For this load case, several designs failed due to large, spanwise, tensile stresses in the crown of the hat-stiffener near the ends of the panel. Furthermore, the STAGS analysis showed that for the two load cases considered in the present analysis, a simple beam analysis provides a good approximation of the stress distribution along the panel length. Since the stress calculations performed using the beam approximation are inexpensive, the approximate beam analysis was used

to calculate the stresses in the crown of the hat-stiffener at 3.5 inches from the panel ends, for all of the 162 structures. The stress results from the approximate beam analysis were compared with the STAGS stress results for 13 structures (points 1-2 and points 16-26 in Table 8). The differences between the simple beam predictions and the STAGS analysis predictions ranged from 0.1% to 6.5%.

Approximate Buckling Analysis. The buckling calculations performed with STAGS for the 25 structures provided in Table 8 showed that for buckling load factors less than one or close to one, buckling was generally local and confined to a single element of the hat-stiffened panel (i.e. only the cap of the hat-stiffener or the panel skin had any appreciable deformation). This observation is demonstrated in Fig. 6, where buckling mode shapes are shown for four design points. The first buckling mode shape for Design Point 3 subjected to combined loading is shown in Fig. 6a. The buckling is mostly confined to the cap of the hat-stiffener in the interior section of the panel. In Fig. 6b, the first buckling mode is shown for Design Point 5, for the internal pressure only load case. For this design and load case buckling is confined mostly to the skin near the panel ends. Figure 6c presents an example of skin buckling in the thin section of the skin near the skin thickness discontinuity**.** Interactive buckling modes were also predicted, but the buckling load factor for these modes were substantially greater than one. An example of an interactive buckling mode is shown in Fig. 6d, where both the cap and the webs of the hat-stiffener buckle together.

Based upon the observations discussed above that the individual components of the stiffened panel buckle independently for buckling load factors close to one, an approximate buckling analysis was developed by representing a subregion of each component of the hat stiffened panel as a simply supported plate. The dimensions of these subregions were found using the width of each element of the stiffener (for example the width $w = 4.3$ *in.* was used for the crown of the hat stiffener) and the length of a half wave of the bucking mode correspond to lowest critical load value of a plate that was simply supported on all edges. The component with the lowest buckling load determined the buckling load for the hat stiffened panel.

The spanwise stresses in the panel induced by the internal pressure load vary quadratically along the length of the panel. However, the stress is approximately constant over a

single buckling half wave, since the length of a single buckling half wave is much smaller than the length of the panel, (see Fig. 6). Therefore, the buckling stress for a single component of the hat stiffened panel was approximated from the buckling solution for a simply supported plate under constant load, that is given by:

$$s_{buck} = \frac{p^2}{t\, m^2 b_b{}^2 R^2} \left[m^4 D_{11} + 2\,(D_{12} + 2\,D_{66})(mnR)^2 + D_{22}(nR)^4 \right] \tag{3}$$

where b_b and t are the width and the thickness of the component of the hat-stiffened panel under consideration, $R = \frac{a_b}{b_b}$ is the ratio between the length and the width of the panel component, and m and n are respectively the number of half waives in the direction parallel and perpendicular to the loading N_x. In appendix A it is shown how the minimum buckling stress for a simply supported plate with fixed width b_b and thickness t is achieved for a length a_b:

$$a_b = \left(\frac{D_{11}}{D_{22}} \right)^{1/4} b_b \tag{4}$$

Substituting Eq. (4), and the the material properties given in Table 1 into Eq. (3), gives the approximate buckling stress for an individual component of the hat-stiffened panel:

$$s_{buck} = 2.25\, 10^8 \left(\frac{t}{b_b} \right)^2 \tag{5}$$

An approximation for the buckling load factor was obtained by dividing the approximate buckling stress given by Eq. (5) by the approximate applied stress, determined from the simple beam analysis discussed above. The approximate buckling load factor is defined as $l = \frac{s_{buckling}}{s_{applied}}$. A value of b_b of 8.0 inches was used in the calculations of s_{buck} for the skin near the ends of the panel and for the skin at the thickness discontinuity ($b - w$, in Fig. 3). To evaluate the buckling stress in the crown of the hat-stiffener, the value of b_b was set to 4.3 inches (w in Fig. 3).

Comparisons of the buckling load factor obtained using the approximate analysis with the buckling load factor predicted by STAGS for the 25 structures indicated that the approximate buckling load factor underestimated the resistance to buckling. This result was to be expected since the neighboring plate elements provide more boundary restraint than is provided by simple support boundary condition. Also the stresses are not constant over the length of a component subregion and the buckling load factor was calculated in the approximate analysis on the basis of the maximum stress over the length a_b. The buckling load factors given by the approximation were up to 75% smaller than the buckling load factors predicted by STAGS. To improve the buckling load factor predictions obtained using the approximate beam-plate analysis the STAGS results were used to fit a scale factor (as a single term response surface) to the buckling load factor in each critical region of the panel. The computed scale factors are provided in Table 9. The combined load condition was critical for buckling for all of the designs considered, so the response surface was generated for this load case only. The buckling load factors predicted by the approximate analysis combined with the scale factors provided in Table 9, had a maximum error of 10% for structures whose buckling modes were mainly localized in one element. The approximate analysis generally overestimated the buckling load factor for structures that showed an interactive buckling mode. These structures had buckling load factors that were well above 1.0.

Minimum Weight Structure. The four three-level design variables, (d, t_{sb}, t_{sb}, t_{cm}) and two-level design variable t_w generate a design domain of 162 points. All 162 designs were analyzed using beam theory to determine the stresses, and the scaled plate-beam approximation to determine the buckling load factor. The most promising design was identified and checked by STAGS analyses. The optimum design, found by inspection of the approximate analysis prediction, is given in Table 10. The structure shown in Table 10 weighs 2.75 lb/ft^2. The maximum spanwise stress predicted by the approximate analysis was 44,101 psi, tension, in the crown of the hat-stiffener, for the pressure-only load condition. The minimum buckling load factor predicted by the approximate analysis was $\lambda = 0.97$ for the combined load condition The design did not exactly satisfy the buckling constraint but it was close enough to evaluate with STAGS

A linear bifurcation analysis for the optimum design in Table 10 was conducted using STAGS. The STAGS linear bifurcation analysis predicted a buckling load factor, $\lambda = 0.93$, and predicted with the same type of buckling mode arises as predicted by the approximate analysis. The buckling mode was predominantly buckling of the skin at the axial location where the cross-section changes. . This buckling load factor corresponds to skin buckling in the interior region of the panel. The maximum predicted tensile stress in the crown of the hat stiffener near the ends was 45,097 psi.

Non-Linear Analysis

A geometrically nonlinear analysis for the optimum design was conducted as a final check on the adequacy of the design. The program computes a nonlinear static solution and then conducts a linear bifurcation analysis with the eigenvalue applied to both loads, the in-plane load and the pressure load. The buckling load factor predicted by the nonlinear analysis was $\lambda = 1.11$. The corresponding buckling mode shown in Fig. 7. The buckling mode is interactive, and the crown and the web of the hat stiffener buckled simultaneously. The interactive buckling predicted by the nonlinear analysis corresponds to the ninth buckling mode predicted by the linear analysis which is 14% higher than the buckling load predicted from the linear prebuckling stress state.

Concluding Remarks

An design study for structural optimization of the upper cover panel of a typical bay of a blended wing body transport alternative to the sandwich one is presented. A hat stiffened laminated composite panel is used in the design. The hat-stiffened panel was subjected to internal pressure load, and to combined internal pressure and in-plane loads. The structural optimization problem was formulated using weight as the objective function, with stress and buckling constraints. The initial optimization was conducted for a design having uniform properties in the axial direction using the PANDA2 program. The design was then refined using a more flexible design procedure

that by combined the STAGS finite element analysis program with response surface approximations for the stresses and for the buckling loads.

The design loads and safety factors were changed during the design process, but the knowledge of the design space gained from the first load case allowed an easy update to the optimum design. Furthermore, in the small region in the design space that was used for updating the design, simple beam and plate approximations could be used with simple correction factors obtained from STAGS.

The design study demonstrated the use of three levels of analysis models and the use of response surface approximations for integrating the analysis models into the design process. This process resulted in reductions in weight for the composite hat stiffener concept from 4.30 lb/ft^2 to 2.75 lb/ft^2. The hat stiffener concept structure proved to be a valid alternative to the sandwich concept since it achieved a weight of less than 3.0 lb/ft^2.

Acknowledgment

This work was supported in part by NASA grants NAG1-1669 and NAG1-2000. Helpful discussions with members of the BWB team, George Rowland, Art Hawley and Professor Peter are gratefully acknowledged. The authors also acknowledge gratefully the useful suggestions and help from Dr. David Bushenell of Lockheed Martin Corporation.

References

1) Mason, B.H., Haftka. R.T., Johnson, E.R., and Farley, G.L., "Variable Complexity Design of Composite Fuselage Frames by Response Surfaces Techniques", Thin Wall Structures 32(4), pp. 235-261, 1998.

2) NASA Contracts NAS1 18862, 20014 and 20546.

3) Bushnell D., "PANDA-program for minimum Weight Design of Stiffened, Composite, Locally Buckled Panels", *Computers and Structures,* **25**, pp 469-605, 1987.

4) Brogen F. A., Rankin C. C. and Cabiness H. D. “STAGS, User Manual Version 3.0”, Lockheed Martin Missiles and Space CO., Inc, Advanced Technology Center, Report Lmms P032594, June 1998.

5) Microsoft Corporation, EXCEL 5.0.

6) Myers R. H., and Montgomery D. C., Response Surface Methodology, Wiley, New York 1995.

7) SAS Institute, “JMP version 3.1”, Cary NC, February 1995.

8) Vitali R., Park P., Haftka R. T., Sankar B. V., ”Structural Optimization of a Hat Stiffened Panel by response Surface Techniques” Proceedings of AIAA/ASME/ASCE/AHS/ASC Structures, Structural Dynamics and Material Conference AIAA Paper -97-1151, April 9-10, 1997 Vol. 4 pp. 2983-2993.

Table 1. Material properties for graphite-epoxy preforms

Design Specifications	Value
E_{11}(msi)	9.25
E_{22}(msi)	4.67
G_{12}(msi)	2.27
ν_{12}	0.397
ε_{all}	$5.40\ 10^{-3}$
σ_{all}(ksi)	50
τ_{all}(ksi)	18
ρ (lb/in^3)	0.0057

Table 2. PANDA2 optimization problem (dimensions in inches)

Objective function : min {weight}	
Design Variables*: b, b_2, w, w_2, h, t_s, t_f, t_w, t_c	
Side Constraints:	
$6 \leq b \leq 24$	(1)
$b_2 - 0.75b \geq 0$	(2)
$4.5 \leq b_2 \leq 18$	(3)
$2 \leq h \leq 6.5$	(4)
$b_2 - w_2 \geq 2.6$	(5)
$2.9 \leq w_2 \leq 15.4$	(6)
$2.25 \leq w \leq 11.75$	(7)
$0.11 \leq t \leq 1.1$	(8)
Buckling and stresses constraints in PANDA2	(9)

*See Fig. 3

Table 3. PANDA2 original and rounded optimum design

Variable	Original	Rounded
Weight (lb/ft^2)	4.65	4.86
b (in.)	13.83	13.83
b_2 (in.)	8.4	8.4
h (in.)	6.5	6.5
w (in.)	4.3	4.3
w_2 (in.)	5.8	5.8
t_s (in.)	0.22	0.22
t_f(in.)	0.34	0.33
t_w(in.)	0.20	0.22
t_c(in.)	0.33	0.33

Table. 4 Design variables used in response surface optimization

variable	Variable meaning
d	Distance from panel ends to thickness discontinuity
t_{sb}	Skin Thickness near panel ends
t_{sm}	Skin Thickness in the interior of the panel
t_{cb}	Crown thickness the near panel ends
t_{cm}	Crown thickness in the interior of the panel

Table 5. Candidate points for response surface construction

Design Variable	Minimum (in.)	Step (in.)	Maximum (in.)	Nominal Design (in.)
d	12	12	48	36
t_{sb}	0.110	0.055	0.440	0.165
t_{sm}	0.110	0.055	0.440	0.110
t_{cb}	0.110	0.055	0.440	0.220
t_{cm}	0.110	0.055	0.440	0.165

Table 6. Initial optimization problem using response surfaces

Objective Function:	Min{weight}
Design Variables:	d, t_{sb}, t_{sm}, t_{cm}, t_{cb}
Constraints:	$\lambda > 1.38$
	$\sigma < 32051$ (psi)
	$t_{sb} - t_{sm} > 0$
	$t_{cm} - t_{cb} > 0$
	$24 < d < 48$ (in.)
	$0.110 < t_{sb} < 0.220$ (in.)
	$0.110 < t_{sm} < 0.165$ (in.)
	$0.165 < t_{cm} < 0.275$ (in.)
	$0.110 < t_{cb} < 0.220$ (in.)

Table 7. Initial optimum design obtained using response surface

Parameter	Optimum
d (in.)	30
t_{sb} (in.)	0.165
t_{sm} (in.)	0.110
t_{cm} (in.)	0.165
t_{cb} (in.)	0.110
Weight (lb/ft^2)	3.533
λ STAGS	1.379
σ (psi.) STAGS	22,450
λ response surface	1.416
σ (psi.) response surface	23,845

Table 8. Structural designs near initial optimum design (number 1)

used for updated response surface optimization

Point #	d (in.)	t_{sb} (in.)	t_{cm} (in.)	t_{cb} (in.)	t_w (in.)	Weight (lb/ft^2)	λ_p	λ_c	σ_{Max} (psi.)
1	30	0.220	0.110	0.110	0.220	3.505	0.848	0.805	56,858
2	30	0.165	0.165	0.165	0.220	3.410	1.680	1.496	46,161
3	30	0.110	0.110	0.110	0.165	2.755	0.661	0.620	-
4	36	0.220	0.220	0.165	0.165	3.366	2.565	1.756	-
5	36	0.220	0.110	0.165	0.165	3.321	0.800	0.695	-
6	36	0.110	0.220	0.165	0.220	3.341	1.000	0.893	-
7	36	0.110	0.220	0.165	0.165	2.943	0.895	0.779	-
8	36	0.110	0.110	0.165	0.220	3.186	0.865	0.797	-
9	36	0.110	0.110	0.165	0.165	2.786	0.761	0.652	-
10	24	0.220	0.220	0.165	0.220	3.602	2.736	1.206	-
11	24	0.220	0.220	0.165	0.165	3.207	2.516	1.003	-
12	24	0.220	0.110	0.165	0.220	3.399	0.870	0.803	-
13	24	0.220	0.110	0.165	0.165	3.002	0.716	0.657	-
14	24	0.110	0.220	0.165	0.220	3.322	1.005	0.906	-
15	24	0.110	0.110	0.165	0.220	3.120	0.832	0.764	-
16	36	0.220	0.165	0.110	0.165	3.290	1.452	1.238	64,761
17	36	0.220	0.110	0.110	0.165	3.212	0.694	0.664	66,607
18	36	0.165	0.220	0.110	0.220	3.553	1.698	1.508	55,149
19	36	0.110	0.110	0.110	0.220	3.189	0.814	0.769	58,858
20	30	0.165	0.165	0.110	0.220	3.420	1.661	1.484	57,009
21	30	0.110	0.220	0.110	0.165	3.334	0.892	0.890	63,389
22	30	0.220	0.220	0.110	0.220	4.000	2.705	1.260	54,627
23	24	0.165	0.110	0.110	0.165	3.262	0.665	0.623	66,618
24	24	0.110	0.220	0.110	0.165	3.324	0.893	0.785	61,609
25	24	0.110	0.220	0.110	0.165	2.926	0.971	0.874	56,235
26	24	0.110	0.110	0.110	0.165	2.722	0.650	0.607	67,113

Table 9. Scale factors for l_c

Buckling Location	Combined load factor
Cap in the interior section	1.804
Skin in the interior section	3.943
Skin at the end section	1.313

Table 10. Minimum weight structure

Design Variable	Value
d (in.)	24.0
t_{sb} (in.)	0.165
t_{cm} (in.)	0.165
t_{cb} (in.)	0.220
t_w (in.)	0.165
Weight	2.755 lb/ft^2

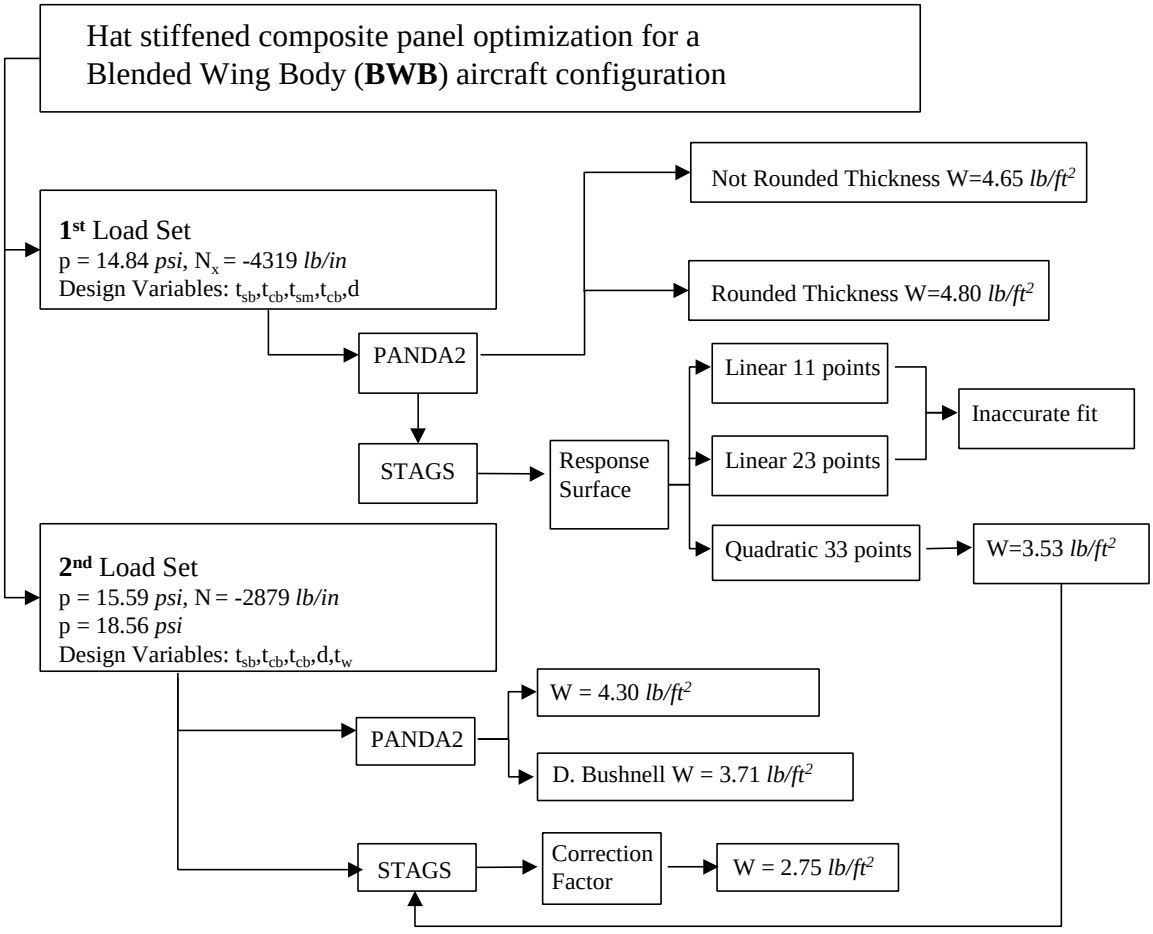

Figure 1A: Flow Chart of the optimization hystory of the hat stiffened panel

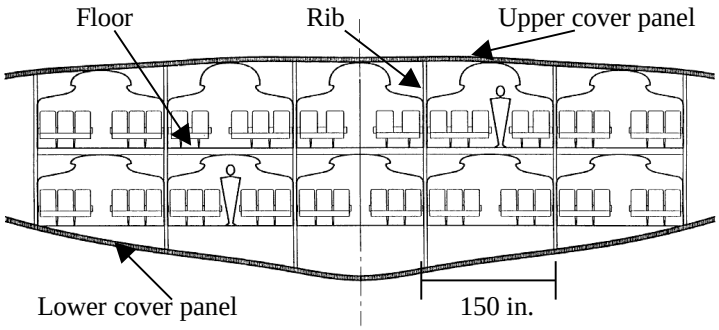

Figure 1. Center-body region of a blended wing body transport airplane

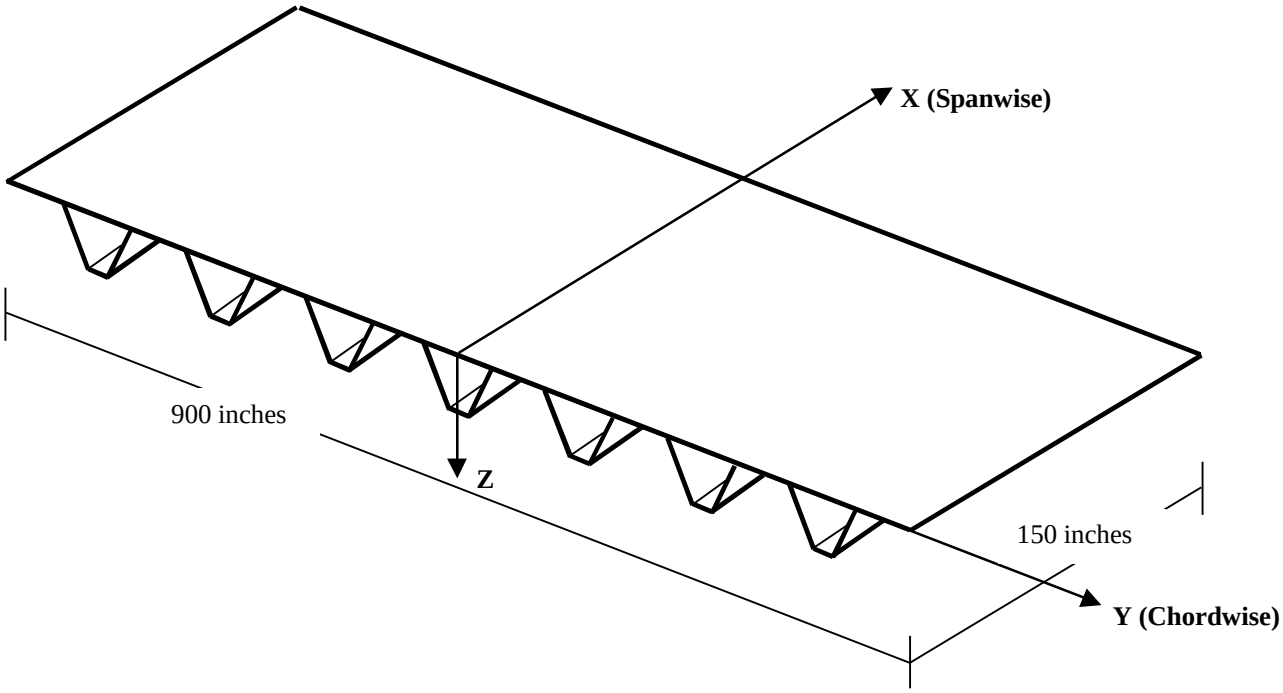

Figure 2. Hat-stiffened skin upper cover panel.

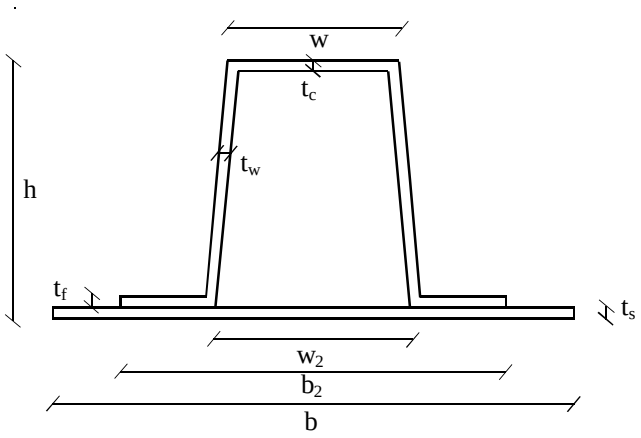

Figure 3. Design variables for the PANDA2 optimization.

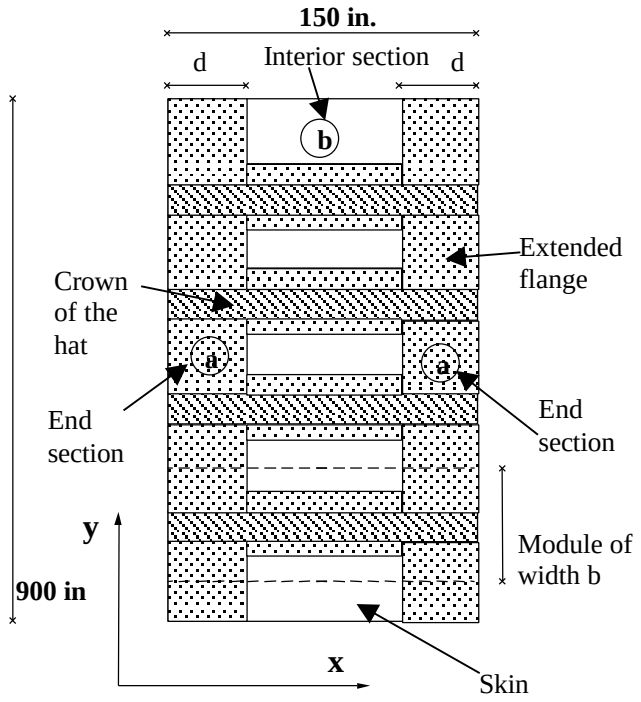

Figure 4. Division of the panel hat-stiffened panel into three sections

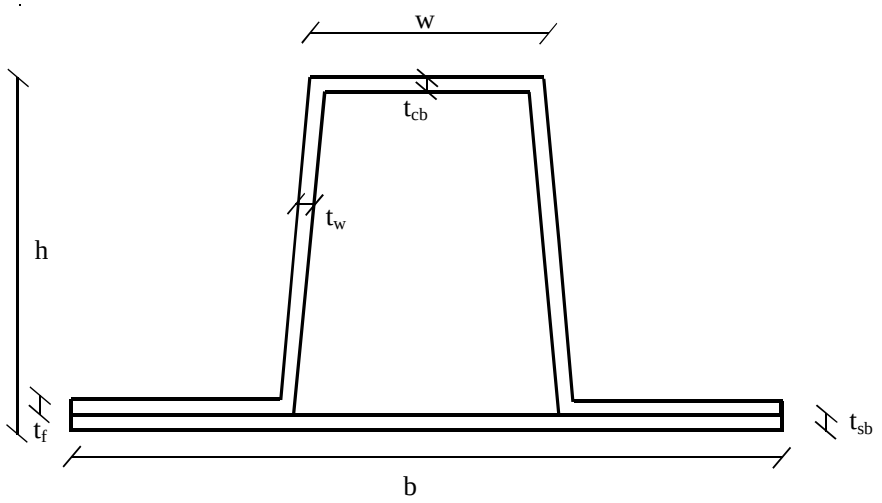

(a) End region

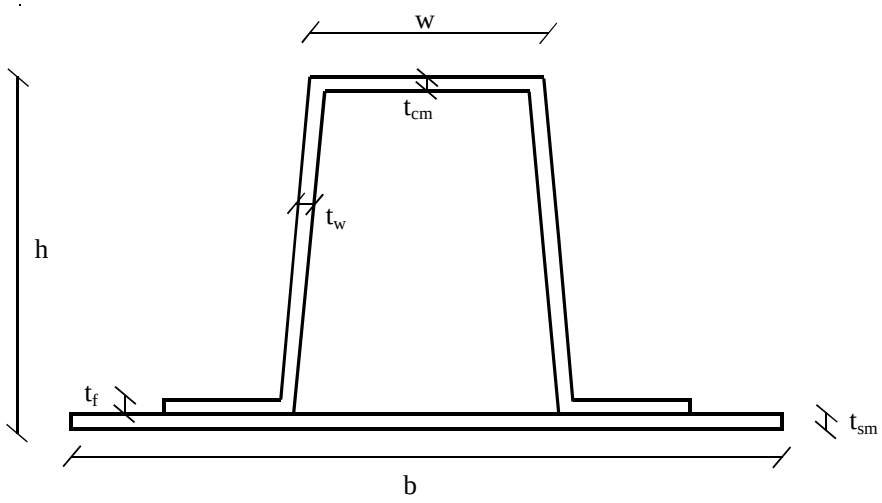

(b) Interior region

Figure 5. Cross-sectional geometry of a variable thickness panel.

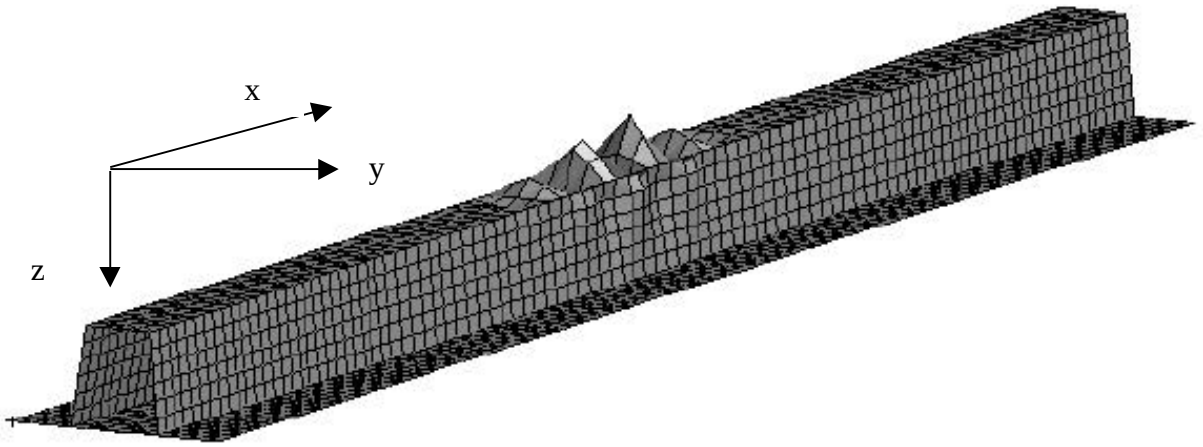

(a) Design Point 3, combined internal pressure and in-plane load case

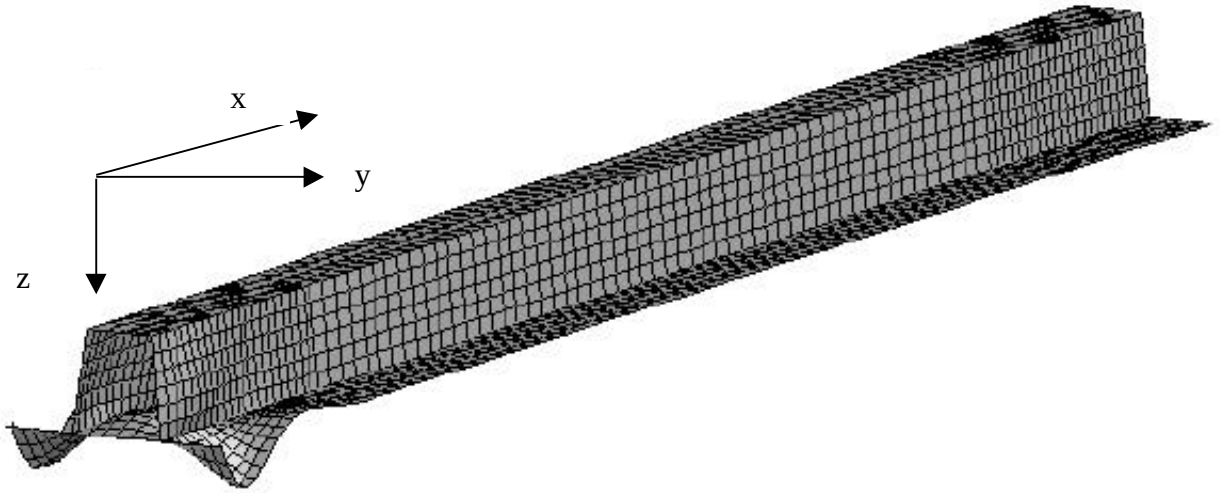

(b) Design point 5, internal pressure load case

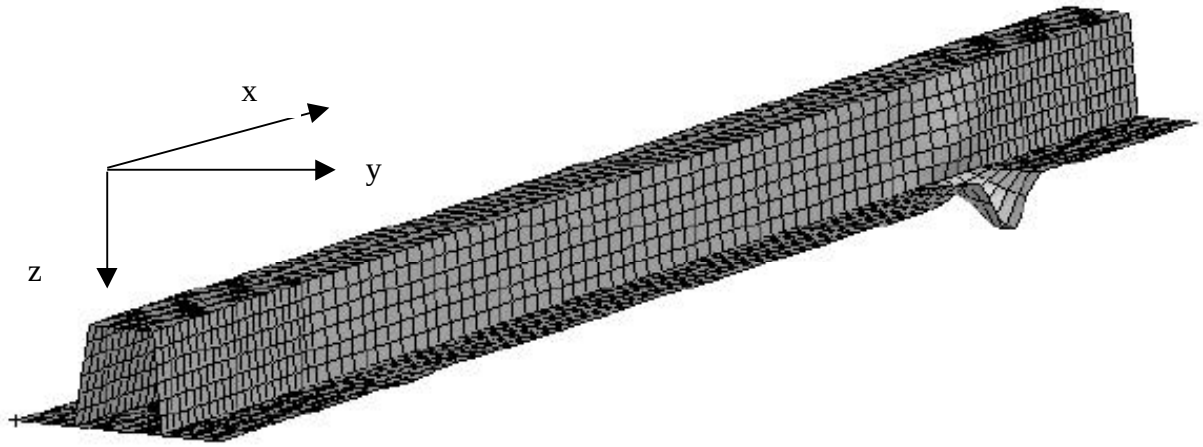

(c) Design point 11, combined internal pressure and in-plane load case

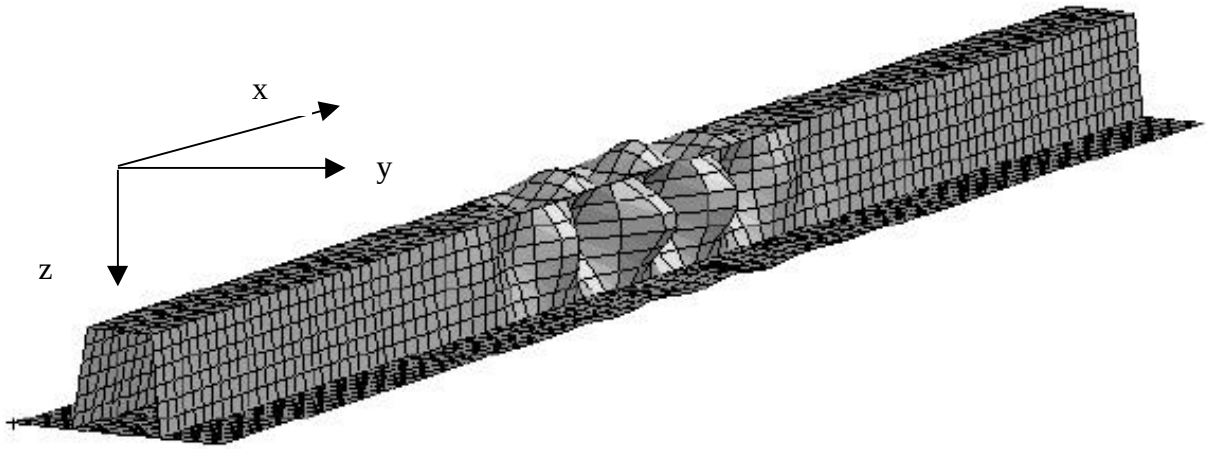

(d) Design point 2, combined load case

Figure 6. Examples of buckling modes predicted by STAGS analyses

(Design point numbers refer to Table 8).

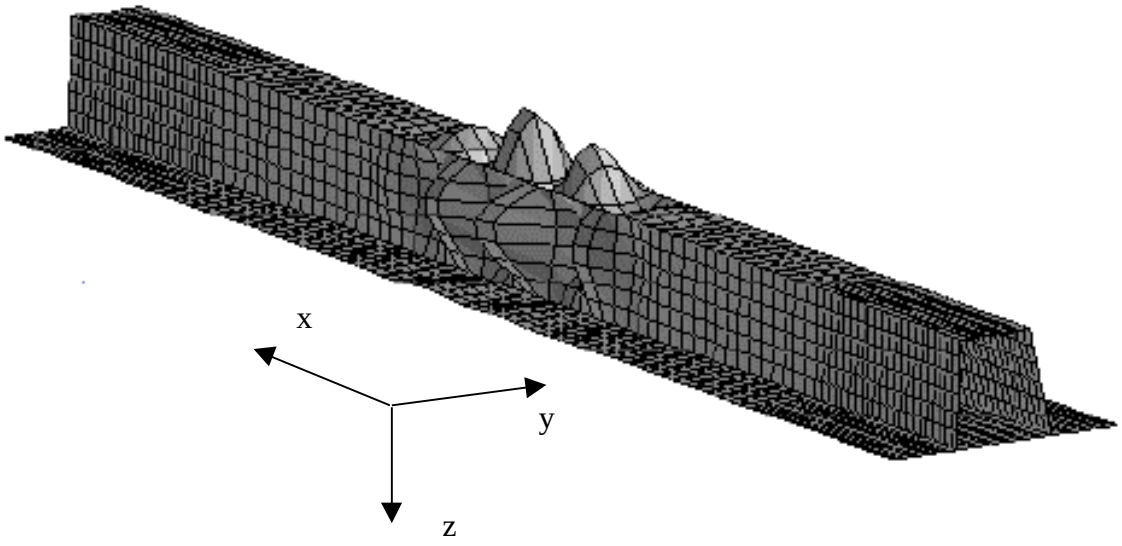

Figure 7. Linear bifurcation buckling analysis prediction from non-linear pre-buckling stresses of optimal design.

Appendix A

The buckling stress of an orthotropic simply supported plate, under a constant compressive stress s_x as shown in Fig. A1 is given by

$$s_{buck} = \frac{p^2}{t\, m^2 b_b{}^2 R^2}\left[m^4 D_{11} + 2(D_{12} + 2\, D_{66})(mnR)^2 + D_{22}(nR)^4\right] \qquad \text{(A6)}$$

where t is the thickness of the plate, $R = \frac{a_b}{b_b}$ is the ratio between the length a_b and the width of the plate b_b. D_{11}, D_{22}, D_{12}, D_{22} are the bending stiffness material properties of the orthotropic plate and n and m are the number of half-waives respectively in the direction perpendicular to the loading and in the direction parallel to the loading.

From Eq. (A1) it is possible to find the length a_b of an orthotropic plate that minimizes s_{buck} for a given width b_b by performing

$$\frac{\partial s_{buck}}{\partial a_b} = 0 \qquad \text{(A7)}$$

which gives

$$a_b = \left(\frac{D_{11}}{D_{22}}\right)^{1/4} \frac{m}{n}\, b_b \qquad \text{(A8)}$$

substituting Eq. (A3) in Eq. (A1) the minimum buckling load s_{buck} is

$$s_{buck} = p^2 n^2 \frac{2\sqrt{D_{11}D_{22}} + 2(D_{12} + 2D_{66})}{t\, b_b^2} \qquad \text{(A9)}$$

The minimum s_{buck} is then obtained for $n = 1$. The fact that s_{buck} in Eq (A4) does not depend on m, suggests that there is an infinite number of plates lengths a_b, one for each value of m in Eq. (A3), for which an orthotropic plate of width b_b achieves its minimum possible buckling load given in Eq. (A4) for $n = 1$. Since the choice of m is free it can be safely chosen as $m = 1$ so that the minimum buckling load s_{buck} for an orthotropic plate of width b_b is

$$s_{buck} = p^2 \frac{2\sqrt{D_{11}D_{22}} + 2(D_{12} + 2D_{66})}{t\, b_b^2} \tag{A10}$$

And it is obtained for a length value

$$a_b = \left(\frac{D_{11}}{D_{22}}\right)^{1/4} b_b \tag{A11}$$